

Effective Feedback Control in Pump Laser Modules Stabilized by Fiber Bragg Gratings

Tomas Pliska, Nicolai Matuschek, and Christoph Harder, *Member, IEEE*

Abstract—On the basis of Jones matrix calculus, we derive an effective reflector model for fiber Bragg grating (FBG) stabilized pump laser modules. This model includes a parameter that takes the effects of varying polarization upon propagation in the fiber into account. This feedback parameter is expressed as a function of the parameters describing the linear and circular birefringence in the fiber. It provides a means for control of the effective feedback received by the pump laser and, hence, for optimization of the pump laser characteristics. Several examples of different fiber arrangements are discussed both theoretically and experimentally regarding their robustness against polarization variation. In general, a combination of twist-induced circular and bend-induced linear birefringence is identified as the cause for loss of effective feedback that ultimately can lead to complete delocking of the laser from the FBG. Guidelines for optimized fiber geometries are given.

Index Terms—External feedback, fiber Bragg grating (FBG), fiber birefringence, pump laser modules, semiconductor lasers.

I. INTRODUCTION

THE PROPERTIES of an erbium-doped fiber amplifier (EDFA) depend on the characteristics of the pump laser diode. Today, fiber Bragg gratings (FBGs) are a standard passive component for wavelength and power stabilization of 980-nm pump lasers [1]–[4]. For maintaining gain flatness over a wide range of operating conditions the light reflected from the FBG locks the laser to the desired narrow wavelength interval defined within the EDFAs absorption band. The most common build technology for FBG stabilized pump laser modules is one that uses a standard single-mode fiber. This approach has proven to be practical and cost-effective in large-scale manufacturing, and several hundreds of thousands of such modules have been deployed in optical networks during the past decade by our company.

The feedback from the FBG is only effective if the light reflected into the semiconductor laser cavity has the proper transverse-electric (TE) polarization. A change of the state of polarization (SOP) upon propagation in the fiber can result in a loss of effective feedback and, in the worst case, complete loss of locking. Such a change of the SOP is, in general, a result of birefringence present in the fiber that is introduced whenever the circular symmetry of the ideal fiber is broken, and an anisotropic refractive-index distribution in the core region is present [5], [6]. Standard single-mode fibers always exhibit some birefringence that is either an inherent property due to material nonuniformity introduced during the fabrication process or a result of some external action on the fiber, such as

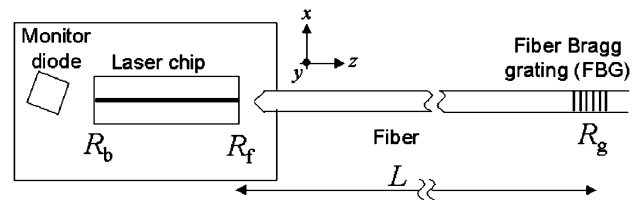


Fig. 1. Schematic of an FBG-stabilized pump laser module (not to scale). R_b , R_f , and R_g denote the back, front, and FBG power reflectivities, respectively. The distance between laser chip and FBG is typically 0.5 to 2 m.

elastic deformations. For FBG-stabilized modules used in EDFAs such deformations result from bending and twisting as the fiber is wound into the EDFA during assembly. For modeling and optimizing the properties of pump modules, it is useful for EDFA designers to understand the influence of the fiber geometry on the effective feedback and, hence, on the electro-optic characteristics of the module. This is particularly important for newly emerging 980-nm pump laser applications such as uncooled modules or high-power temperature-stabilized modules for “one-for-two-replacement” pump schemes in EDFAs with increasingly stringent requirements on performance, especially regarding power and wavelength stability [7]–[9].

This paper is based on two previous publications of ours that discuss the effective reflector model for pump lasers [10] and the effect of changing polarization due to fiber birefringence on pump module characteristics [11]. Here, we will combine the results derived in these two articles and include the fiber birefringence into the effective reflector approach. In particular, we will derive a parameter in the expression for the effective front reflectivity of the compound cavity (the feedback parameter) that includes all effects of fiber birefringence. On the basis of this model, we will discuss means of feedback control and the robustness against polarization change of various fiber pigtail arrangements.

II. FBG-STABILIZED PUMP LASER DIODES

A schematic of an FBG-stabilized pump laser diode is shown in Fig. 1. The laser cavity is formed by its front and back mirrors with power reflectivities R_f and R_b , respectively. The light emitted through the front facet is coupled into the fiber with efficiency T_c . In the most common scheme, an antireflection coated lens fabricated on the fiber tip is used for optimizing the coupling efficiency. The light propagates along the fiber and is reflected by a Bragg reflector of reflectivity R_g positioned at a distance of 0.5 to 2 m from the laser. The resonator defined by the laser front mirror and FBG is referred to as the external cavity. In commonly

Manuscript received November 17, 2004; revised June 14, 2005.

The authors are with Bookham (Switzerland) AG, CH-8045 Zürich, Switzerland (e-mail: tomas.pliska@bookham.com).

Digital Object Identifier 10.1109/JSTQE.2005.853842

used pump modules, R_f and R_g take values of 0.01 to 0.1, and R_b is higher than 0.9. Description of this multiple cavity system is simplified by combining the laser front facet and FBG into an effective reflector with a compound effective front reflectivity R_{eff} [10]. Thereafter, it is usually sufficient to consider the cavity formed by the effective front reflector and the laser back facet, whereas all other optical cavities may be neglected.

A typical index-guided narrow-stripe InGaAlAs/GaAs semiconductor laser emits light linearly polarized along the TE direction. Hence, only TE-polarized light reflected from the FBG into the laser cavity effectively contributes to locking. Extending the expression given in [10] by including a parameter f , we can write the compound front reflectivity R_{eff} as

$$R_{\text{eff}} = R_f + T_c^2(1 - R_f)^2 \frac{fR_g}{1 - R_f R_g} \approx R_f + T_c^2 f R_g \quad (1)$$

where the approximation holds, since $R_f \ll 1$ and $R_f R_g \ll 1$.

The influence of the effective reflectivity on the pump laser properties, such as light-current characteristics, threshold current, and spectral properties, has been discussed in [10]–[12]. The feedback parameter f can be viewed as a measure of the polarization preserving properties of the fiber loop. In what follows, we will show that it is indeed possible to introduce a feedback parameter according to (1), and we will derive its relation to the fiber's birefringence. In particular, we will show that f is in good approximation equal to the normalized power carried in the TE-polarization of the light reflected into the laser cavity.

According to the approximate expression given in (1) the effective front reflectivity is written as the sum of a contribution from the laser cavity (laser front facet) and a contribution of the external cavity (fiber and FBG). It is important to realize that the spectral dependencies of R_f and R_g are very different. Whereas in standard pump lasers the front mirror reflectivity is spectrally flat over several tens of nanometers in the 980-nm region, the FBG reflectivity has a sharply peaked maximum with a width on the order of one nm within the erbium's absorption line. Therefore, if the dominant contribution comes from the second addend, the properties of the pump laser are governed by the FBG, and the laser is locked to the FBG. On the other hand, if R_f dominates, the laser tends to behave as if it were freely running without being influenced by the reflection from the FBG. Examples of emission spectra for these two states are shown in [11, Fig. 4].

Equation (1) is valid for incoherent power-wise addition of the multiple reflections in the external cavity. Most pump lasers deployed in EDFAs are preferentially operated in a multimode state of emission for which an incoherent calculation is appropriate. In this case, low-frequency power fluctuations in the kilohertz-regime are strongly suppressed, whereas high-frequency noise, above approximately 50 kHz, is of no concern for pumping EDFAs, as it is filtered by the erbium's slow response.

III. FIBER BIREFRINGENCE

Bend and twist are the two geometrical deformations usually imposed on the fiber when mounting it into an EDFA. Controlled

bending is necessitated by space constraints in the EDFA housing, whereas twist is more likely to be induced accidentally as a parasitic effect when coiling the fiber into loops.

A bent fiber receives stress in the direction of the bend radius which causes uniaxial linear birefringence with the fast extraordinary axis e in the plane of the bend (parallel to the bend radius) and the slow ordinary axis o perpendicular to this plane [13]. The bend-induced birefringence in a fiber is then given by

$$\Delta n_l \equiv n_e - n_o = -a \left(\frac{r}{R} \right)^2 \quad (2)$$

where n_e and n_o represent the extraordinary and ordinary refractive indices, respectively, r denotes the radius of the fiber (core and glass cladding, usually $r = 62.5 \mu\text{m}$ for standard single-mode fibers), R is the bend radius, and a contains the elastic and photo-elastic material constants [13].

A twist of the fiber introduces shearing stress and produces circular birefringence resulting in a pure rotation of any input SOP [14]. Thus, a linearly polarized input will remain linearly polarized, while the output polarization may be rotated with respect to the input. The circular birefringence Δn_c is given by

$$\Delta n_c \equiv |n_l - n_r| = \frac{\lambda}{2\pi} g\tau. \quad (3)$$

The refractive indices for left and right circular polarization are denoted by n_l and n_r , respectively, while τ is the twist rate (in units of rad/m). The constant g contains the material parameters.

Both circular and linear birefringence are represented by unitary matrices $\mathbf{R}(\alpha)$ and $\mathbf{M}(\Phi, \theta)$ in the Jones matrix formalism [15]

$$\mathbf{R}(\alpha) = \begin{pmatrix} \cos \alpha & -\sin \alpha \\ \sin \alpha & \cos \alpha \end{pmatrix} \quad (4)$$

$$\mathbf{M}(\Phi, \theta) = \begin{pmatrix} \cos \frac{\Phi}{2} + i \sin \frac{\Phi}{2} \cos 2\theta & i \sin \frac{\Phi}{2} \sin 2\theta \\ i \sin \frac{\Phi}{2} \sin 2\theta & \cos \frac{\Phi}{2} - i \sin \frac{\Phi}{2} \cos 2\theta \end{pmatrix} \quad (5)$$

where $\alpha = g\tau z/2$ is the resulting rotation angle of the plane of polarization, $\Phi = 2\pi\Delta n_l z/\lambda$ is the linear phase shift and the angle θ the orientation of the phase plate's principal axes relative to the laboratory frame.

Any arbitrary sequence of several retardation plates and rotators can be represented by a simple product of an effective rotator and an effective linear phase plate [16]

$$\mathbf{A}_{\text{eff}} = \mathbf{M}(\Phi_{\text{eff}}, \tilde{\theta}_{\text{eff}}) \mathbf{R}(\alpha_{\text{eff}}) \equiv \begin{pmatrix} A & B \\ -B^* & A^* \end{pmatrix}. \quad (6)$$

Therefore, a fiber exhibiting circular and linear birefringence can be represented by the unitary matrix \mathbf{A}_{eff} . The parameters Φ_{eff} , $\tilde{\theta}_{\text{eff}}$, and α_{eff} represent an effective (net) phase shift, orientation angle, and rotation, respectively. (Alternatively, a sequence of unitary transformations may be described by the product $\mathbf{R} \cdot \mathbf{M}$, resulting in different effective parameters but otherwise identical general results.)

For analyzing the resonator formed by the laser front facet and the FBG, we make use of the fact that the backward propagation is represented by the transposed matrix $\mathbf{A}_{\text{eff}}^T$. Then, by using

the basic calculation rules for \mathbf{R} and \mathbf{M} , we find the effective matrix for one round-trip

$$\mathbf{A}_{\text{eff}}^T \mathbf{A}_{\text{eff}} = \mathbf{M}(2\Phi_{\text{eff}}, \tilde{\theta}_{\text{eff}} - \alpha_{\text{eff}}) \equiv \mathbf{M}_{\text{eff}}(2\Phi_{\text{eff}}, \theta_{\text{eff}}). \quad (7)$$

\mathbf{M}_{eff} represents a linear phase plate with twice the effective phase shift acquired in one pass and an effective orientation $\theta_{\text{eff}} = \tilde{\theta}_{\text{eff}} - \alpha_{\text{eff}}$ with respect to the laboratory frame. For multiple round-trips, the effective matrix is given by the n th power of the single round-trip matrix (5)

$$\mathbf{M}_{\text{eff}}^n(2\Phi_{\text{eff}}, \theta_{\text{eff}}) = \mathbf{M}(2n\Phi_{\text{eff}}, \theta_{\text{eff}}). \quad (8)$$

IV. EFFECTIVE FRONT FACET REFLECTIVITY AND FEEDBACK PARAMETER

For deriving an expression for the effective front reflectivity including the effect of birefringence, we calculate the Jones vector \mathbf{u}_2 representing the reflected SOP at the laser front facet

$$\mathbf{u}_2 = \mathbf{u}_0 + \sum_{n=1}^{\infty} \mathbf{u}_2^{(n)} \equiv \begin{pmatrix} u_{2,x} \\ u_{2,y} \end{pmatrix} \quad (9)$$

with

$$\mathbf{u}_0 = r_{f+} \hat{e}_x \quad (10)$$

$$\mathbf{u}_2^{(n)} = t_f^2 t_c^2 r_g^n r_{f-}^{n-1} e^{2in\varphi} \mathbf{M}_{\text{eff}}^n \hat{e}_x \quad (11)$$

where \hat{e}_x is the linearly TE-polarized normalized output SOP defining the x -direction of the laboratory frame (Fig. 1), and $\mathbf{u}_2^{(n)}$ is the Jones vector of the light just passing the laser front facet after n round-trips in the external cavity. The phase φ is given by $\varphi = 2\pi n_{\text{fib}} L / \lambda$, with n_{fib} being the mean refractive index of the fiber. In general, the reflection coefficients r_{f+} , r_{f-} , and r_g , the transmission coefficient t_f , as well as the coupling efficiency t_c , are complex numbers referring to field amplitudes. Here, they are assumed to be polarization-independent. The front facet reflection coefficients seen from inside the laser cavity r_{f+} and seen from the external cavity r_{f-} generally have different phases. The corresponding coefficients with respect to power are given by

$$\begin{aligned} |r_{f+}|^2 &= |r_{f-}|^2 = R_f \\ |r_g|^2 &= R_g \\ |t_f|^2 &= T_f = 1 - R_f \\ |t_c|^2 &= T_c. \end{aligned} \quad (12)$$

Using (8), we then find the normalized Jones vector $\hat{\mathbf{u}}_2^{(n)}$ at the front facet after n round trips

$$\begin{aligned} \hat{\mathbf{u}}_2^{(n)} &\equiv \mathbf{M}_{\text{eff}}^n \hat{e}_x \\ &= \begin{pmatrix} \cos(n\Phi_{\text{eff}}) + i \sin(n\Phi_{\text{eff}}) \cos(2\theta_{\text{eff}}) \\ i \sin(n\Phi_{\text{eff}}) \sin(2\theta_{\text{eff}}) \end{pmatrix}. \end{aligned} \quad (13)$$

In the incoherent case, one adds up powers from multiple round trips in the external cavity. The effective reflectivity can be defined as the power carried in the TE-component of the vector

\mathbf{u}_2 given in (9). As a result of some lengthy manipulation of (8)–(13), we find, for the effective front reflectivity, the expression

$$\begin{aligned} R_{\text{eff}} &= |r_{f+}|^2 + \sum_{n=1}^{\infty} |u_{2,x}^{(n)}|^2 = R_f + T_c^2 (1 - R_f)^2 \frac{R_g}{1 - R_f R_g} \\ &\quad \times \left(1 - \sin^2 2\theta \sin^2 \Phi \right. \\ &\quad \left. \times \left(1 + \frac{R_f R_g (1 + 2 \cos 2\Phi - R_f R_g)}{1 - 2R_f R_g \cos 2\Phi + (R_f R_g)^2} \right) \right) \end{aligned} \quad (14)$$

where we have omitted the subscripts for the net phase shift and orientation angle. (The expression for the coherent case is given in the Appendix.) By comparing to (1), we immediately realize that

$$\begin{aligned} f &= 1 - \sin^2 2\theta \sin^2 \Phi \\ &\quad \times \left(1 + \frac{R_f R_g (1 + 2 \cos 2\Phi - R_f R_g)}{1 - 2R_f R_g \cos 2\Phi + (R_f R_g)^2} \right). \end{aligned} \quad (15)$$

Noticing that $R_f R_g \ll 1$ (typically $R_f R_g$ is on the order of $10^{-4} - 10^{-2}$) for common reflectivities of 980-nm pump lasers, we can rewrite (15) as

$$f = f^{(1)} + \delta f \quad (16a)$$

$$f^{(1)} = 1 - \sin^2 2\theta_{\text{eff}} \sin^2 \Phi_{\text{eff}} \quad (16b)$$

where $f^{(1)}$ represents the first round-trip feedback parameter. In most practical cases in which the laser is locked to the FBG, the dominant contribution to f comes from the first round-trip in the external cavity, whereas higher order reflections only add a small correction δf . Therefore, $f \approx f^{(1)}$ is usually a valid approximation. Moreover, by setting $n = 1$ in (13) and by comparing to (16b), we find

$$f^{(1)} = \left| \hat{u}_{2,x}^{(1)} \right|^2. \quad (17)$$

For a discussion of the feedback parameter, we first consider some particular cases. If the fiber acts as an equivalent $\lambda/2$ -plate ($\Phi_{\text{eff}} = 0, \pi, 2\pi, \dots$) or if θ_{eff} is a multiple of $\pi/2$, i.e., one of the principal birefringence axes oriented parallel to the TE-direction $\hat{\mathbf{u}}_0$, then, according to (15), f takes its maximum value of 1. In this case, all the Jones vectors \mathbf{u}_0 and $\mathbf{u}_2^{(n)}$, as well as the resulting reflected vector \mathbf{u}_2 , are parallel to the TE-direction. On the other hand, if the fiber can be represented by an equivalent $\lambda/4$ -plate ($\Phi_{\text{eff}} = \pi/2, 3\pi/2, 5\pi/2, \dots$) oriented at $\theta_{\text{eff}} = \pi/4$, the SOPs $\hat{\mathbf{u}}_2^{(n)}$ alternate between TE-polarization and its orthogonal transverse-magnetic (TM) counterpart for even and odd n , respectively. As a result f is always larger than $R_f R_g / (1 + R_f R_g) > 0$, implying that the feedback never vanishes completely. For the first round-trip, however, we find $f^{(1)} = 0$ for this case. Thus, in good approximation, f can be considered as a parameter taking values between 0 and 1. Finally, (17) states that the feedback parameter is in good approximation equal to the TE-polarized fraction of the total power at the laser facet after the first round-trip.

The importance of (14) to (17) is given by the fact that the effect of varying polarization state is now included in

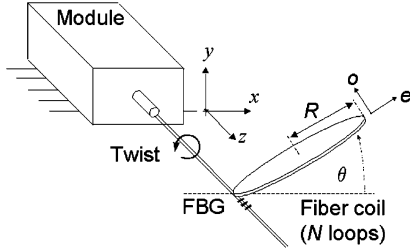


Fig. 2. Basic pump module arrangement with the fiber coiled into N loops of radius R . The fiber represents a linear waveplate with the fast (extraordinary) and slow (ordinary) axes denoted by e and o , respectively. The waveplate can be rotated by an angle θ out of the xz plane of the laboratory frame.

the expression for the compound front reflector. Equation (15) gives an explicit expression for this feedback parameter. Generally, f is a function of the four parameters R_f , R_g , θ_{eff} , and Φ_{eff} . However, in the first round-trip approximation (16b), the feedback parameter is only a function of the two parameters describing the birefringence present in the fiber: the phase shift Φ_{eff} quantifying the induced and intrinsic linear birefringence and the angle θ_{eff} that includes the orientation of this linear birefringence and the effect of the twist applied to the fiber.

We have discussed a method for practical determination of the feedback parameter earlier in [11] and shown that, again, in the first round-trip approximation, the feedback parameter is generally related to the properties of the SOP at the FBG $\hat{u}_1^{(1)}$ by

$$f^{(1)} = \left(\frac{e^2 - 1}{e^2 + 1} \right)^2 \quad (18)$$

where $e = a/b$ is the ellipticity of $\hat{u}_1^{(1)}$. (a and b denote the long and short half axis of the ellipse, respectively.) Equation (18) is derived by using elementary relations between the Jones vectors $\hat{u}_1^{(1)}$ and $\hat{u}_2^{(1)}$. In particular, it shows that if $\hat{u}_1^{(1)}$ is a linear SOP ($e = \infty$), $f^{(1)}$ is unity, whereas for $\hat{u}_1^{(1)}$ being a circular SOP ($e = 1$), $f^{(1)}$ vanishes.

V. BASIC CONFIGURATIONS WITH FIBER LOOPS REPRESENTING WAVEPLATES

The most simple mounting configuration for a pump module is one in which the fiber is looped N times into a coil of radius R as shown in Fig. 2. The fiber coil represents a linear phase plate that can be used for manipulating the polarization of the light propagating in the fiber [17], if other birefringence, e.g., in the fiber attachment to the module can be neglected. In this section, we will discuss the feedback parameter for two cases: one in which polarization change arises mainly from a rotation of the fiber coil out of the xz plane of the laboratory frame (i.e., a change of the orientation θ of the waveplate's axes relative to the laboratory frame) while twist between module and coil remains weak, and one in which the coil remains in the xz plane (i.e., with the fast extraordinary axis parallel to the TE-polarized output SOP of the laser) while strong twist acts on the fiber section between module and FBG.

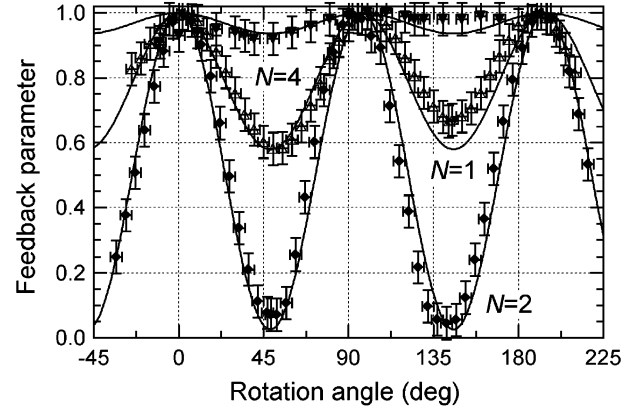


Fig. 3. Feedback parameter as a function tilt angle θ using the experimental arrangement shown in Fig. 2. Lines represent the calculation according to (20) for $N = 1, 2$, and 4 fiber loops, respectively (other parameters are given in the text). Open triangles, solid diamonds, and solid triangles indicate measured data.

The linear phase difference between the two orthogonal polarization components acquired upon propagation through the fiber loop is given by

$$\Phi = -\frac{(2\pi r)^2}{\lambda R} aN. \quad (19)$$

The configuration shown in Fig. 2 with the fiber coil being rotated around the z axis can be described by a sequence of a polarization rotator followed by a linear phase shifter, as described by (6), with $\tilde{\theta}_{\text{eff}} = \theta$, $\Phi_{\text{eff}} = \Phi$ given by (19), and $\alpha_{\text{eff}} = g\theta/2$ being the polarization rotation angle induced by the twist on the fiber section between module and coil. According to (16b), the feedback parameter is then given by

$$f^{(1)} = 1 - \sin^2 \left(2\theta \left(1 - \frac{g}{2} \right) \right) \sin^2 \left(\frac{(2\pi r)^2}{\lambda R} aN \right). \quad (20)$$

The feedback parameter as a function of rotation angle θ for three different waveplate configurations is shown in Fig. 3 for a Corning HI1060 fiber with $r = 62.5 \mu\text{m}$, $R = 2.9 \text{ cm}$, and $N = 1, 2$, and 4 , and $\lambda = 980 \text{ nm}$. The solid lines indicate calculations using the material parameters $a = 0.13$ [13] and $g = 0.146$ [14]. According to (19), the respective fiber loops correspond to waveplates with phase shifts of 0.22π , 0.45π , and 0.90π , respectively, i.e., approximately $\lambda/8$ -, $\lambda/4$ -, and $\lambda/2$ -waveplates. The good agreement between calculation and measurement indicates that the aforementioned values for a and g are valid in this case.

In most common EDFA designs, the fiber coil is arranged in the plane of the housing that corresponds to the xz plane of our laboratory frame. In this case, the fast axis of the coil is parallel to x , and one expects that the incident linear SOP is parallel to this axis. Hence, the SOP should remain linear upon propagation through the coil always yielding $f = 1$ for any phase shift acquired. However, this is no longer true if twist is present in the fiber section between laser and loop. In this situation with θ taking values of $\theta = m\pi$ with $m = 0, 1, 2, \dots$, the initial TE-polarized SOP from the laser is rotated as the light propagates through the twisted fiber section between laser and coil. As a result the linear SOP arriving at the coil is generally no longer

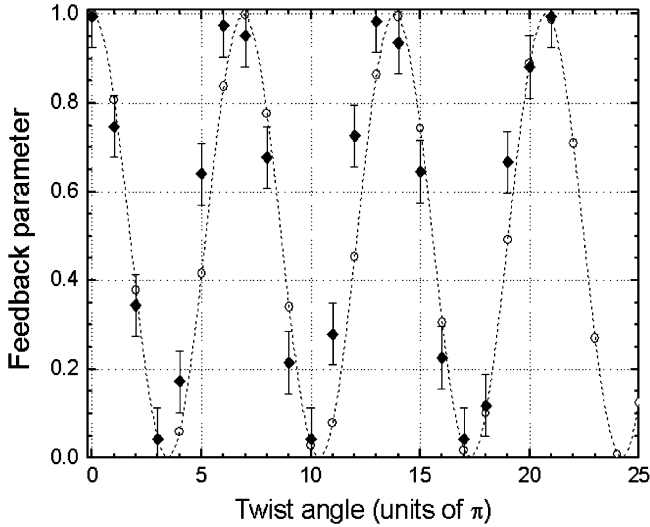


Fig. 4. Measured (solid diamonds) and calculated (open circles and dashed line) effective feedback of a FBG stabilized module with a fiber wound into a $\lambda/4$ -waveplate. The section between laser and FBG is rotated by multiples m of π around the fiber axis such that $\theta = m\pi$ (Fig. 2).

parallel to one of the coil's principal axes but rotated by an angle $\alpha_{\text{eff}} = gm\pi/2$. In practice, this second scenario can occur if the fiber is first looped into a coil, and then, during mounting into the EDFA housing, this coil is accidentally or intentionally rotated around the fiber axis in the section between module and coil.

A measurement representative of this second case is shown in Fig. 4. The full diamonds indicate the measured feedback parameter for a fiber coil approximately equivalent to a $\lambda/4$ -waveplate ($\Phi = \pi/2$). Twist in the fiber section between laser and coil is induced by rotating the coil in multiples m of π , while the coil remains in the xz plane. Open circles are calculated for the respective angles $\theta = m\pi$ with $0 \leq m \leq 25$. The dashed line merely connects these points. As expected for a $\lambda/4$ -waveplate, the feedback parameter oscillates between 0 and 1, indicating that this twist-induced rotation of the SOP can cause a variation of the feedback parameter as strong as the one resulting from the previously discussed orientational change of the fiber coil. For small m that are most likely to occur in a manufacturing environment, the feedback parameter drops to $f = 0.81$ for $m = 1$, $f = 0.38$ for $m = 2$ and as low as $f = 0.04$ for $m = 3$. In other words, if the coil is rotated 1.5-times around the fiber axis, the feedback parameter can almost completely vanish. This illustrates the importance of careful fiber handling that avoids twist when mounting a module with a fiber wound in a coil into an EDFA.

VI. SUPERPOSITION OF SEVERAL BIREFRINGENCE TYPES

In Section V, we have discussed the situation in which two different birefringence mechanisms appear sequentially along the fiber, while in a given fiber section, only one type of birefringence is present. In what follows, we shall allow for a superposition of several birefringence types in an otherwise homogeneous fiber.

For all following examples, we assume that the fiber is looped into a circular coil of radius R while twist of rate τ

is simultaneously applied to the fiber during coiling. Three different superposed birefringence mechanisms are taken into account: 1) a bend-induced ("strong") linear birefringence Δn_i oriented at an angle θ_i relative to the laboratory frame, 2) a parasitic ("weak") linear birefringence Δn_p oriented at an angle θ_p , and 3) a circular birefringence producing a rotation of polarization per unit length of $\rho = g\tau/2$. Notice that the intrinsic parasitic birefringence of single-mode fibers can exceed 10^{-7} , the same value that is obtained for the induced birefringence in a loop of 7-cm radius.

The case of several superposed birefringence mechanisms can be treated by integration of differential Jones matrices [18], [19]. As a result of this procedure, we obtain, for the propagation between laser and FBG, the matrix

$$\mathbf{A} = \begin{pmatrix} \cos QL + iS \frac{\sin QL}{Q} & (-\rho + iC) \frac{\sin QL}{Q} \\ (\rho + iC) \frac{\sin QL}{Q} & \cos QL - iS \frac{\sin QL}{Q} \end{pmatrix} \quad (21)$$

with

$$S = \frac{\pi}{\lambda} (\Delta n_i \cos 2\theta_i + \Delta n_p \cos 2\theta_p) \quad (22a)$$

$$C = \frac{\pi}{\lambda} (\Delta n_i \sin 2\theta_i + \Delta n_p \sin 2\theta_p) \quad (22b)$$

$$Q = (S^2 + C^2 + \rho^2)^{1/2}. \quad (22c)$$

Notice that \mathbf{A} takes the same general form as the matrix \mathbf{A}_{eff} in (6) so that all relations for the feedback parameter f derived in Section IV are also valid for the case of superposed birefringence mechanisms. By calculating the Jones vector $\hat{\mathbf{u}}_2^{(1)}$ and by using (17), we obtain the first round-trip feedback parameter

$$f^{(1)} = 1 - \left(\frac{C}{Q} \sin 2QL + \frac{2\rho S}{Q^2} \sin^2 QL \right)^2. \quad (23)$$

The mathematical condition for polarization control is contained in (22): Whenever $\Delta n_i \gg \Delta n_p$ and $\Delta n_i \gg \rho\lambda/\pi$, the induced birefringence will dominate all parasitic effects.

For assessing the robustness of the fiber loop against polarization change, it is useful to define a lower limit below which the feedback parameter is not allowed to drop, for example, $f = 0.5$. A suitable means for evaluating the tolerance against twist is to analyze the dependence of the feedback parameter on fiber length. This function oscillates whereby the modulation depth increases with growing twist rate. An example is shown in Fig. 5 for a circular fiber coil arranged in the xz plane of the laboratory frame ($\theta_i = 0$) and a bend radius of 3 cm, with the twist rate as a parameter. The respective induced birefringence is 5.6×10^{-7} . Parasitic linear birefringence is supposed to vanish. For a twist rate of 6.3 (2π) rad/m (1 full turn/m), the feedback parameter does not drop below 0.75, whereas at 25 (8π) rad/m, the feedback parameter can completely vanish.

In Fig. 6, we plot the calculated dependence of the feedback parameter on the bend radius for a fiber length of 1 m, and twist rates of 6.3, 18.9, and 62.8 rad/m, and $\theta_i = 0$. Again, parasitic birefringence is supposed to vanish. For sufficiently strong induced birefringence, i.e., for small bend radii, the feedback parameter is close to unity. Resonant coupling to the

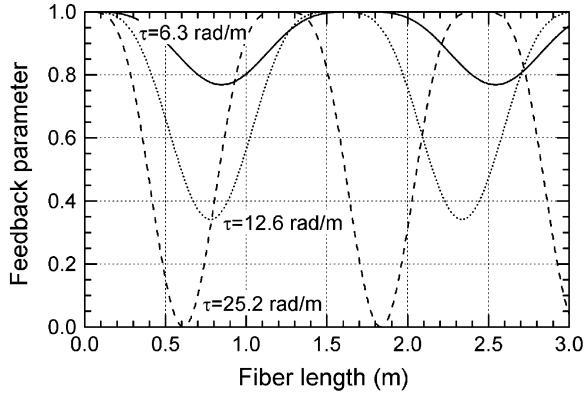


Fig. 5. Calculated feedback parameter as a function of fiber length for a fiber submitted to uniform bend and twist, assuming a circular fiber coil arranged in the xz plane ($\theta_i = 0$) with a loop radius of 3 cm. Parasitic linear birefringence is supposed to vanish (twist rates as indicated).

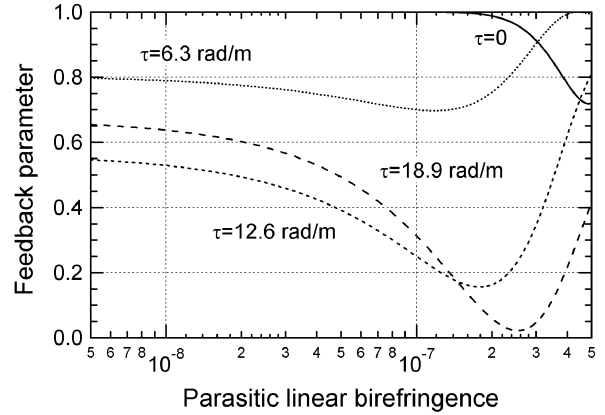


Fig. 7. Feedback parameter as a function of parasitic linear birefringence for a fiber loop of 3-cm radius ($\Delta n_i = 5.6 \times 10^{-7}$, $\theta_i = 0$) and different twist rates as indicated in the graph. The parasitic linear birefringence is oriented at an angle of 0.62π in this example and the fiber length is 1 m.

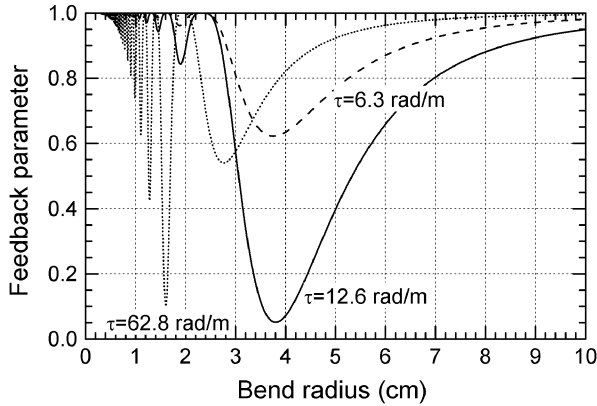


Fig. 6. Calculated feedback parameter as a function of bend radius for a fiber submitted to uniform twist, assuming a circular fiber coil arranged in the xz plane ($\theta_i = 0$). The fiber length is 1 m. Twist rates are as indicated in the graph.

orthogonal polarization mode occurs whenever circular and linear birefringence are of the same magnitude ($\Delta n_i \approx \lambda\rho/\pi$), setting an upper limit to the useful coil radius. For the particular fiber length of 1 m, the feedback parameter does not drop below 0.6 for any bend radius at a twist rate of 6.3 rad/m, whereas at a twist rate of 12.6 rad/m, the feedback parameter drops below 0.5 at a radius of 3 cm. The dotted curve with $\tau = 62.8$ rad/m is a useful example despite the high twist rate, as it illustrates how twist applied during looping can reduce the feedback parameter. If a fiber pigtail of 1 m is wound into a coil of 10 loops with 1.6 cm radius, applying a twist of 2π per loop, the twist rate is exactly 62.8 rad/m. For this particular loop radius and twist rate, the feedback parameter takes a value as small as ~ 0.1 . A similar effect of cross-coupling between orthogonal polarization modes due to a periodic perturbing birefringence is mentioned in [6].

In Fig. 7, we plot the calculated dependence of the feedback parameter as a function of parasitic birefringence oriented at $\theta_p = 0.62\pi$, which is approximately worst case) for uniform twist rates of 0, 6.3, 12.6, and 18.9 rad/m. The coil radius is 3 cm ($\Delta n_i = 5.6 \times 10^{-7}$), and the fiber length is 1 m. Whereas for a twist rate of 6.3 rad/m the feedback parameter remains higher than 0.7, it shows a considerably stronger variation for

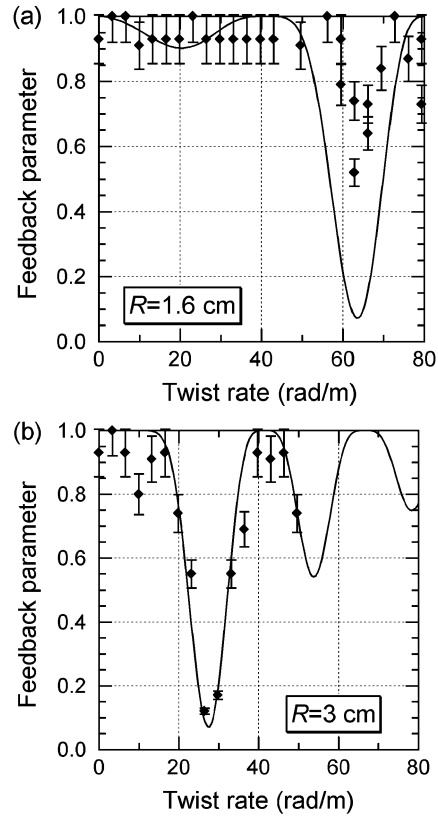


Fig. 8. Measured (diamonds) and calculated (lines) feedback parameter as a function of twist rate applied to the fiber (length 2 m) looped into a coil of (a) 1.6- and (b) 3-cm radius ($\theta_i = 0$). The data are taken with an FBG in a *Corning* HI1060 single-mode fiber.

twist rates of 12.6 and 18.9 rad/m, indicating that the induced linear birefringence no longer effectively counteract, the parasitic linear and circular birefringence.

The increasing robustness of the feedback parameter against twist with decreasing bend radius is reflected in Fig. 8(a) and (b). We have realized measurements of the feedback parameter using an apparatus that enabled us to apply a controlled twist rate to the fiber of 2-m length while looping it into a coil of defined

radii of 1.6 and 3 cm. Solid lines indicate the calculated dependence, assuming that parasitic linear birefringence is negligible ($\Delta n_p = 0$). Clearly, the feedback parameter is much less sensitive to twist for $R = 1.6$ cm than for $R = 3$ cm. Notice that the general trends of measurement and calculation are in good agreement. At high twist rates, which are rather unlikely to occur in practice, accurate control of the torque applied to the fiber makes precise control of the birefringence difficult. Moreover, small parasitic nonuniformities along the fiber in combination with a high twist rate and small bend radius can have a strong impact on feedback parameter control. This explains the deviations between measurement and calculation in this regime.

VII. CONCLUSION

Including a feedback parameter into the effective reflector model for FBG stabilized pump lasers with TE-polarized output enables us to quantify the effects of linear and circular birefringence on the effective feedback and, ultimately, on the pump laser characteristics. This feedback parameter can be easily measured by analyzing the ellipticity of the SOP at the location of the FBG [11], [12].

Generally, it is a combination of twist and linear birefringence that causes coupling to the orthogonal TM-polarization and, thus, a reduction of effective feedback into the laser cavity. The strategy for controlling the polarization in the fiber loop is to induce a strong linear birefringence that dominates any parasitic birefringence and to fix its axes properly. Such a situation is obtained if the fiber is looped into a circular coil located in the xz plane. A circular fiber arrangement is clearly more robust than oval, elliptical, or rounded-rectangular fiber geometries. In these latter cases, there is no induced birefringence mechanism that counteracts parasitic birefringence on the weakly bent or straight sections of fiber. The robustness against twist and intrinsic birefringence decreases as bend radius and fiber length increase. As a guideline, the coil radius should not exceed 4 cm for a fiber length of 1–1.5 m, if a tolerance for twist of 6.3 rad/m (1 full turn/m) and intrinsic birefringence of 10^{-7} is to be maintained. Because of the quadratic growth of induced birefringence with decreasing coil radius, considerable improvements in robustness are obtained by relatively small reductions of the coil radius. The practical lower limit for the loop radius is imposed by fiber reliability, fiber handling, geometrical constraints, etc., and is typically 1.5 to 2 cm. Ultimately, an optimized fiber loop arrangement is designed by finding a balance between these various parameters.

Having discussed the two cases of sequential arrangement of two different birefringent elements (rotator followed by linear phase plate) as well as superposition of several birefringence mechanisms in a uniform fiber (twist and bend), we conclude on the importance of minimizing parasitic effects, in particular, twist. In an ideal fiber arrangement twist is completely eliminated. Practically, the FBG parameters are chosen in such a way that locking is maintained for a feedback parameter as low as 0.1. In combination with the guidelines outlined in this article, this gives a sufficient margin for cost-effective large-scale manufacturing of EDFAs.

APPENDIX

For deriving an expression for the effective front reflectivity in the coherent case for amplitude-wise addition of round-trips in the external cavity, we make use of (8) to (13). Again, after some lengthy calculation, we obtain

$$R_{\text{eff}} = |u_{2,x}|^2 = \left| r_{f+} + \sum_{n=1}^{\infty} u_{2,x}^{(n)} \right|^2 = \left| \frac{r_{f+} + t_f^2 t_c^2 r_g e^{2i\varphi} (\cos \Phi + i \sin \Phi \cos 2\theta) - r_g r_{f-} e^{2i\varphi}}{1 - 2r_g r_{f-} e^{2i\varphi} \cos \Phi + r_g^2 r_{f-}^2 e^{4i\varphi}} \right|^2 \quad (\text{A1})$$

where Φ and θ indicate a net phase and a net orientation angle, respectively. An amplitude feedback parameter \tilde{f} can then be expressed as

$$\tilde{f} = \frac{(1 - r_g r_{f-} e^{2i\varphi})(\cos \Phi + i \sin \Phi \cos 2\theta - r_g r_{f-} e^{2i\varphi})}{1 - 2r_g r_{f-} e^{2i\varphi} \cos \Phi + r_g^2 r_{f-}^2 e^{4i\varphi}}. \quad (\text{A2})$$

ACKNOWLEDGMENT

The authors would like to thank H. Richard for valuable technical assistance. They also wish to express their gratitude to Prof. A. Hardy from the University of Tel-Aviv, Tel-Aviv, Israel, as well as to Dr. L. Thévenaz from the École Polytechnique Fédérale, Lausanne, Switzerland, for very helpful discussions on the subject of this work.

REFERENCES

- [1] K. O. Hill, Y. Fujii, D. C. Johnson, and B. S. Kawasaki, "Photosensitivity in optical fiber waveguides: Application to reflection filter fabrication," *Appl. Phys. Lett.*, vol. 32, no. 10, pp. 647–649, May 1978.
- [2] C. R. Giles, T. Erdogan, and V. Mizrahi, "Simultaneous wavelength-stabilization of 980-nm pump lasers," *IEEE Photon. Technol. Lett.*, vol. 6, no. 8, pp. 907–909, Aug. 1994.
- [3] B. F. Ventruco, G. A. Rogers, G. S. Lick, D. Hargreaves, and T. N. Demayo, "Wavelength and intensity stabilisation of 980 nm diode lasers coupled to fibre Bragg gratings," *Electron. Lett.*, vol. 30, no. 25, pp. 2147–2149, Dec. 1994.
- [4] T. Pliska, S. Mohrdiek, and C. Harder, "Power stabilisation of uncooled 980 nm pump laser modules from 10 to 100 °C," *Electron. Lett.*, vol. 37, no. 1, pp. 33–34, Jan. 2001.
- [5] J.-I. Sakai and T. Kimura, "Birefringence and polarization characteristics of single-mode optical fibers under elastic deformations," *IEEE J. Quantum Electron.*, vol. QE-17, no. 6, pp. 1041–1051, Jun. 1981.
- [6] S. C. Rashleigh, "Origins and control of polarization effects in single-mode fibers," *J. Lightwave Technol.*, vol. LT-1, no. 2, pp. 312–331, Jun. 1983.
- [7] B. Schmidt, N. Lichtenstein, B. Sverdlov, N. Matuschek, S. Mohrdiek, T. Pliska, J. Müller, S. Pawlik, S. Arlt, H.-U. Pfeiffer, A. Fily, and C. Harder, "Further development of high power pump laser diodes," in *Proc. SPIE Int. Symp. Inform. Technol. Commun.*, Orlando, FL, 2003.
- [8] S. Mohrdiek, T. Pliska, R. Bättig, N. Matuschek, B. Valk, J. Troger, P. Mauron, B. E. Schmidt, I. D. Jung, C. S. Harder, and S. Enochs, "400 mW uncooled MiniDIL pump modules," *Electron. Lett.*, vol. 39, no. 15, pp. 1105–1107, Jul. 2003.
- [9] T. Pliska, S. Arlt, R. Bättig, T. Kellner, I. Jung, N. Matuschek, P. Mauron, B. Mayer, S. Mohrdiek, J. Müller, S. Pawlik, H.-U. Pfeiffer, B. Schmidt, B. Sverdlov, S. Teodoropol, J. Troger, B. Valk, and C. Harder, "Wavelength stabilized 980 nm uncooled pump laser modules for erbium-doped fiber amplifiers," *Opt. Lasers Eng.*, vol. 43, no. 3–5, pp. 271–289, Mar./May 2005.

- [10] M. Achtenhagen, S. Mohrdiek, T. Pliska, N. Matuschek, C. S. Harder, and A. Hardy, "L-I characteristics of fiber Bragg grating stabilized 980-nm pump lasers," *IEEE Photon. Technol. Lett.*, vol. 13, no. 5, pp. 415–417, May 2001.
- [11] T. Pliska, N. Matuschek, S. Mohrdiek, A. Hardy, and C. Harder, "External feedback optimization by means of polarization control in fiber Bragg grating stabilized 980-nm pump lasers," *IEEE Photon. Technol. Lett.*, vol. 13, no. 10, pp. 1061–1063, Oct. 2001.
- [12] N. Matuschek, T. Pliska, B. Sverdlov, S. Mohrdiek, B. Schmidt, and C. Harder, "Polarization effects in wavelength-stabilized pump laser modules," in *Proc. 15th Annu. Meeting IEEE Lasers Electro-Optics Soc.*, Glasgow, U.K., 2002.
- [13] R. Ulrich, S. C. Rashleigh, and W. Eickhoff, "Bending-induced birefringence in single-mode fibers," *Opt. Lett.*, vol. 5, no. 6, pp. 273–275, Jun. 1980.
- [14] R. Ulrich and A. Simon, "Polarization optics of twisted single-mode fibers," *Appl. Opt.*, vol. 18, no. 13, pp. 2241–2251, Jun. 1979.
- [15] R. C. Jones, "A new calculus for the treatment of optical systems. I. Description and discussion of the calculus," *J. Opt. Soc. Amer.*, vol. 31, pp. 488–493, Jul. 1941.
- [16] H. Hurwitz Jr. and R. C. Jones, "A new calculus for the treatment of optical systems. II. Proof of three general equivalence theorems," *J. Opt. Soc. Amer.*, vol. 31, pp. 488–499, Jul. 1941.
- [17] H. C. Lefèvre, "Single-mode fibre fractional wave devices and polarisation controllers," *Electron. Lett.*, vol. 16, no. 20, pp. 778–780, Sep. 1980.
- [18] R. C. Jones, "A new calculus for the treatment of optical systems. VII. Properties of the N-matrices," *J. Opt. Soc. Amer.*, vol. 31, p. 671, Aug. 1948.
- [19] S. Huard, *Polarization of Light*. New York: Wiley, 1997.

Tomas Pliska was born in Prague, Czech Republic, in 1967. He received the Diploma degree in physics and physical chemistry and the Ph.D. degree in physics from the Swiss Federal Institute of Technology (ETH), Zurich, Switzerland, in 1992 and 1997, respectively. His Ph.D. research was in nonlinear optics and integrated optics in ferroelectric materials.

From 1998 to 1999, he was with the Center for Research and Education in Optics and Lasers/CREOL, University of Central Florida, Orlando, where he conducted research in nonlinear integrated optics in polymers. Since November 1999, he has been with JDS Uniphase, Nortel Networks, and Bookham (Switzerland) AG, Zurich, where he is involved in the development of pump laser chips and modules.

Nicolai Matuschek was born in Biberach/Riss, Germany, in 1968. He received the Diploma degree in physics from the University of Ulm, Ulm, Germany, in 1995 and the Ph.D. degree from the Swiss Federal Institute of Technology (ETH) Zurich, Switzerland, in 1999. His Ph.D. research was in the theory and design of optical interference coatings for femtosecond solid-state lasers.

Since December 1999, he has been with JDS Uniphase, Nortel Networks, and Bookham (Switzerland) AG, Zurich, where he is currently involved in modeling and simulation of high-power semiconductor diode lasers.

Dr. Matuschek is a member of the German Physical Society.

Christoph Harder (M'82) received the Diploma, Master EE, and Ph.D. degrees from the Swiss Federal Institute of Technology (ETH) Zurich, Switzerland, in 1979 and Caltech, Pasadena, CA, in 1980 and 1983, respectively.

He is Director, Research and Development of the High Power Laser Diode group of Bookham Technology at the facility in Zurich. He was co-founder and leader of the R&D effort of the IBM Zurich Laser Diode Enterprise, which pioneered the first 980-nm high-power pump laser for telecom applications. Over the last few years, his research group has expanded into the field of 14xx telecom pumps as well as 808 and 9xx multimode pumps for industrial applications. He has published more than 100 papers and 20 patents and has held a variety of staff and management position at Caltech, IBM, Uniphase, JDS Uniphase, Nortel, and now Bookham.

Dr. Harder has served as General Chair at the International Semiconductor Laser Conference and at the LEOS Annual Meeting and on numerous technical program and steering committees.